Throughput-Optimized Adaptive Transmission Power Control for BLE in Dynamic Environments

Ziyao Zhou[1], Hen-Wei Huang[1,2]

GLOBECOM 2025 - 2025 IEEE Global Communications Conference | 979-8-3315-7781-0/25/$31.00 ©2025 IEEE | DOI: 10.1109/GLOBECOM59602.2025.11431749

***Abstract*—In dynamic environments, Bluetooth Low Energy (BLE) data throughput often exhibits significant fluctuations. To counteract this instability, transmission power (TXP) is commonly configured at its maximum level—an approach that, while improving data throughput, substantially increases energy consumption. This study introduces a closed-loop TXP control strategy that utilizes a Proportional-Integral-Derivative (PID) controller, deployed at a central device to dynamically regulate the TXP of peripheral devices. The proposed method aims to optimize energy consumption while ensuring the required data throughput. The relationship between Received Signal Strength Indicator (RSSI) and throughput was thoroughly analyzed under varying environmental conditions, demonstrating that environmental factors critically influence throughput stability. Subsequently, comprehensive assessments of power consumption, throughput, and the central device's RSSI were performed by varying the TXP setting. In distance-varying scenarios (0–50 meters), the PID-controlled system maintained a throughput of around 400 kbps while reducing peripheral power consumption by 4.4 times compared to fixed 8 dBm TXP operation. Furthermore, compared to a fixed -10 dBm TXP configuration, the PID controller sustained throughput above application requirements with the same power consumption level, achieving an optimal balance between energy efficiency and communication reliability.**

***Index Terms*—PID, BLE, Wireless Communication, Data Throughput, Power Consumption**

I. Introduction

Bluetooth Low Energy (BLE) technology has become increasingly prevalent in the Internet of Things (IoT) field [1]–[4], driven by its low power consumption and suitability for multiple communication applications. It has a maximum data throughput of 2 Mbps, and power consumption is about 10 mW [5].

One major challenge in BLE is that the data throughput can easily be affected by ambient environments. Throughput is the net rate at which application data is successfully delivered over a connection [6]. As illustrated in Figure 1, throughput variations in longer distances show a decreasing trend. The throughput is influenced by three components: path loss, noise floor, and channel effect [7]. These factors introduce fluctuations, making throughput inherently unstable.

To ensure a high quality of service, the BLE system's throughput should exceed the specific demands of the target application, thereby guaranteeing stable communication performance. For example, BLE Audio implementations employing the low complexity communication codec (LC3) require data rates up to 320 kbps with 10-millisecond frame intervals [8], while human motion tracking typically demands approximately 80 kbps when sampling at 100 Hz [9]. Generally, the user selects the highest transmission power (TXP) to overcome throughput fluctuation. However, these methods significantly compromise the energy efficiency.

[1]School of Electrical and Electronic Engineering, Nanyang Technological University, Singapore
[2]LKC School of Medicine, Nanyang Technological University, Singapore
ZHOU0557@e.ntu.edu.sg
henwei.huang@ntu.edu.sg

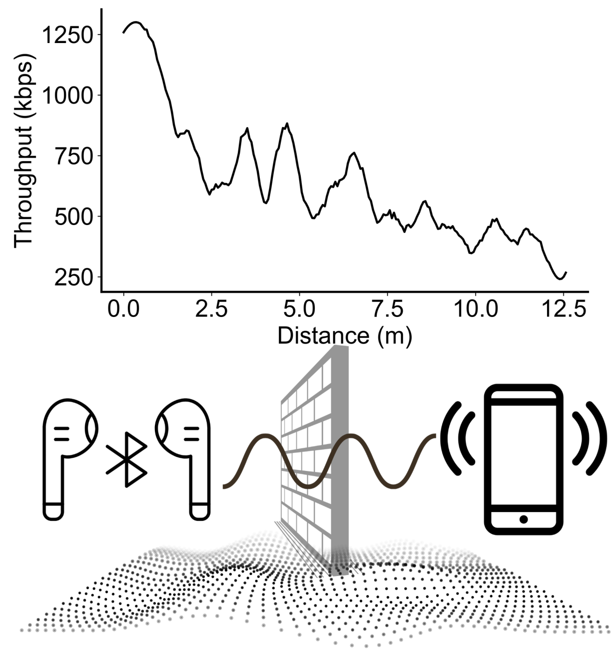

Fig. 1: Throughput variation versus distance for indoor BLE communications (transmission power = 0 dBm). The changes in throughput are caused by path loss, the noise floor, and channel effects.

Several algorithms have been proposed to maintain communication throughput while improving BLE's energy efficiency. One of the most relevant is AdaptaBLE [10], which regulates TXP based on the Packet Reception Ratio (PRR). However, it relies on accumulating packet-loss statistics, leading to slow responsiveness. Another new method is described in [11], making use of both Received Signal Strength Indicator (RSSI) and PRR information to tune the TXP. Though RSSI is a fast-update parameter that could compensate for the latency of PRR to some extent, it is considered an unreliable metric due to its inherent inaccuracies in reflecting channel quality [12]. In addition, the same RSSI under different environments has a different influence on the throughput [13].

Both algorithms indirectly regulate throughput, employing non-robust BLE TXP control strategies based on conditional judgment. Although throughput is the most intuitive communication metric, no study has directly utilized calculated throughputs for TXP control.

In this study, we propose a closed-loop TXP control strategy that employs a Proportional-Integral-Derivative (PID) controller, deployed on the central device. The controller dynamically regulates the TXP of the peripheral device by utilizing the throughput computed at the central device. This method is designed to minimize power consumption on the peripheral side while maintaining sufficient data throughput for specified applications. This study elucidates the correlation between RSSI and throughput in various environments, provides a detailed analysis of throughput, power consumption, and RSSI across different TXP settings, and evaluates the effectiveness of the PID controller in enhancing both throughput stability and energy efficiency.

II. Methodology

The methodology began with an analysis of the relationship between RSSI and data throughput, followed by an examination of power consumption, throughput, and RSSI across various TXP levels. Subsequently, we implemented a closed-loop control system based on a PID controller, which dynamically adjusts the TXP in response to real-time throughput feedback.

A. Relationship between RSSI and Throughput under Different Environments

We utilized two nRF54L15 devices as the experimental platform. One device was configured as the central device, responsible for acquiring real-time RSSI and throughput values, while also receiving data for the target application. At the same time, the other functioned as the peripheral device, continuously transmitting a 244-byte string. Data exchange between the two Nordic devices was conducted via the Nordic UART Service (NUS).

The experiments employed the following communication parameters:

- ATT MTU size: 498 bytes
- Connection interval: 320 units (400 ms)
- Physical layer (PHY) data rate: 2 Mbps

Real-time RSSI measurements on the central device were obtained using the nRF Connect SDK's built-in function. The nRF54L15 updates RSSI values within 20 microseconds upon signal level changes [14], giving the fast-updated value.

However, calculating throughput requires a time window, and the choice of this calculation interval can affect the measured throughput, as BLE communication is inherently a discrete, packet exchange process rather than a continuous one.

In detail, the throughput was calculated as follows: each time the central device received a data packet, it accumulated the length of the data packet received. Once the system timer exceeded the optimal interval, the total accumulated data length was used to compute the throughput for that interval. The counter was then reset, and the device proceeded to store data for the next interval.

To find the optimal interval, we selected five different throughput calculation intervals—10000 ms, 1000 ms, 100 ms, 10 ms, and 1 ms—in the first experiment. The TXP for this experiment is 8 dBm, and the distance between the central and peripheral devices is 9 m indoors. This setup enabled us to evaluate how the granularity of throughput measurement affects the accuracy of the throughput calculation result.

The second experiment was conducted across three distinct environments: the indoor laboratory, the corridor, and the rooftop. The indoor laboratory posed the most challenging conditions for BLE communication, characterized by a high density of electronic equipment and furniture that introduced substantial electromagnetic interference and signal attenuation. The corridor, although it avoided active electronic devices, still had moderate complexity due to multipath reflections and scattering along the walls. In contrast, the rooftop provided the cleanest environment, offering an open and unobstructed space with minimal interference, thereby serving as the ideal reference setting for performance evaluation.

During the experiment, the peripheral device was kept stationary, while the central device was mounted on a movable platform, allowing for a controlled change in the distance between them. Seven target RSSI levels, ranging from –20 to –80 dBm, were selected. The platform was moved to achieve an RSSI value close to each target level, at which point it remained stationary for one minute. During this interval, both RSSI and throughput variations were recorded for analysis.

B. Power Consumption, Throughput and RSSI with Varying TXP

The power consumption of a BLE device is directly influenced by its TXP and data rate [10]. The nRF54L15 used in the study supports a configurable output power of up to +8 dBm, with a fine resolution of 1 dB step sizes from –10 dBm to +8 dBm [14]. The resolution provided by the nRF54L15 is shown in Table I. In comparison, the nRF52833 also offers the highest TXP to +8 dBm, but with coarser 4 dB step increments [15]. This comparison highlights the significantly higher resolution of the nRF54 series in TXP control.

TABLE I: TXP Setting Resolution

Output-Power Range (dBm)	Step Size (dB)	Number of Steps
+8 to –10	1	18
–10 to –22	2	6
–22 to –28	6	1
–28 to –40	12	1
–40 to –46	6	1

We employed the same software setup as in the previous experiments to evaluate power consumption under continuous sending conditions, with optimal intervals for calculating throughput.

The peripheral and central devices were placed 9 m away indoors to conduct the test. The peripheral device was powered using a Nordic Power Profiler Kit II (PPK), which served

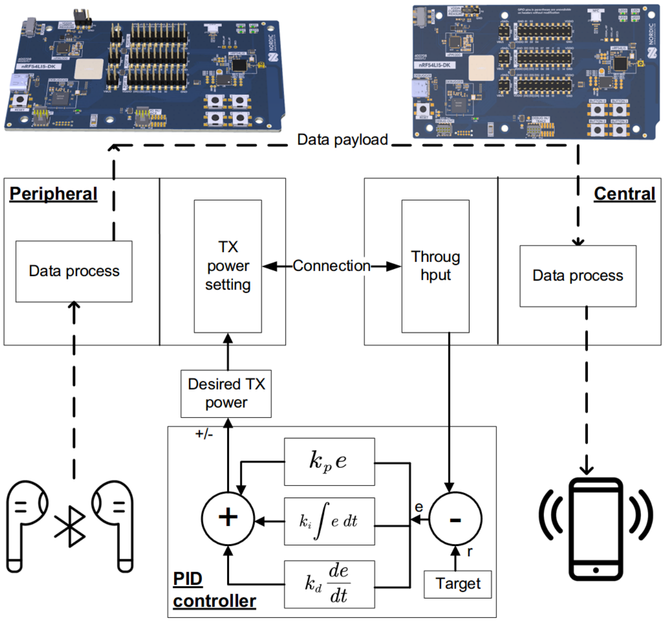

Fig. 2: Block Diagram of the PID Controller. Dashed lines indicate data transmission paths, and solid lines represent the PID closed-loop control loop.

as an external power source supplying a stable 1.8 V for emitter. Simultaneously, it enabled high-resolution current measurements with a sampling rate of 100,000 samples per second, ensuring accurate characterization of the device's energy consumption. The central device continuously logs the receiver's RSSI at a specified TXP.

This environment included shelves and electrical appliances, introducing potential signal scattering and attenuation, and simulating a realistic static testing scenario. With a 9-meter testing distance, packet loss rates typically rise, potentially leading to connection failures and intermittent radio inactivity. In this scenario, we could check whether changing TXP will affect overall throughput, power consumption, and how it will affect the central device's RSSI.

C. PID Controller Deployment

The proposed PID control framework employs a dual-loop architecture, as illustrated in Figure 2. The outer loop, represented by dashed lines, manages data generation, transmission, and processing, which is the primary function of BLE communication.

The inner loop, indicated by solid lines, constitutes the closed-loop PID control mechanism. Within this loop, the central device continuously monitors throughput, the PID controller computes the appropriate TXP for subsequent communication, and adjusts the peripheral device's TXP accordingly. All control logic and processing are executed on the central device to minimize computational load and energy consumption on the peripheral device.

The adjustable TXP range was set between -46 dBm and +8 dBm, corresponding to the full configurable range supported by the nRF54L15 [14]. Although the device offers a fine resolution of 1 dB steps within the –10 dBm to +8 dBm range, output power remains adjustable below –10 dBm as well, albeit with reduced resolution. The detailed resolution is shown in the previous Table I.

We utilized the proportional (P) and integral (I) parameters for control regarding the PID controller. The peripheral and central devices were placed in fixed positions under consistent environmental conditions for the parameter selection. By tuning the parameters, we identified the optimal values that maintained the target number and minimized the standard deviation of the throughput, specifically $k_p = 0.000009$, $k_i = 0.0000001$, and $k_d = 0$ with a target of 400,000 bps. This target value exceeds the 320 kbps throughput of LE Audio, thereby providing a safety margin. Additionally, we set the PID output limit to 3, ensuring that the system quickly converges to the target value without excessive overshoot. The PID frequency is set to the same one as the optimal throughput calculation frequency.

The peripheral device was then mounted on a platform and gradually moved away from the central device at a constant velocity of 0.3 m/s within the dynamic corridor environment for three times. This configuration emulated a dynamic communication scenario in which signal strength gradually deteriorates with increasing distance. The PPK continuously measured the peripheral device's power consumption throughout the experiment while the central device recorded a real-time throughput log. This setup enabled a comprehensive assessment of how PID adjustments influenced both energy usage and communication throughput. The primary objective was to evaluate the PID controller's capability to optimize TXP and sustain reliable throughput adaptively under varying conditions.

III. Results and Discussion

A. Relationship between RSSI and Throughput under Different Environments

In the first experiment, we set the TXP to 8 dBm with a distance of 9 meters between the central device and the peripheral device, both of which were located indoors. The PID calculation is disabled; we independently investigated the impact of calculation frequency on the computed throughput results. We measured throughput at five different frequencies—0.1 Hz (10 s), 1 Hz (1 s), 10 Hz (100 ms), 100 Hz (10 ms), and 1000 Hz (1 ms). The experimental results are summarized in Figure 3.

The observation is that throughput instability has two sources: one is inherent fluctuation, and the other is the calculation interval. To be more specific, higher calculation frequencies led to more significant deviations in measurement results. Specifically, throughput calculated at 0.1 Hz exhibited the highest stability with a standard deviation of 55.65, whereas significant fluctuations emerged at 1000 Hz with a standard deviation of 911.72. We also observed that when the frequency exceeds 10 Hz, the median value deviates significantly from the mean. Increasing the frequency leads to a higher incidence of outliers, thereby exacerbating the divergence between the median and the mean. Given our aim to achieve throughput measurements that are both stable and sensitive enough to capture rapid variations caused by factors such as interference and distance, we selected a calculation frequency of 1 Hz as the optimal frequency for throughput calculation.

Figure 4 illustrates the relationship between data throughput and RSSI. The colors red, green, and blue correspond to the indoor laboratory conditions, the corridor environment, and the rooftop scenario, respectively. Overall, higher RSSI values—indicative of better signal quality—correlate with higher and more stable data throughput across all three environments. For instance, when the RSSI reaches approximately –20 dBm, all three cases exhibit stable RSSI and throughput, with throughput reaching around 1300 kbps.

Comparative analysis indicates that both RSSI and data throughput exhibit greater variability and instability in complex environments. This is reflected in the broader distribution of RSSI values and more pronounced fluctuations in throughput at comparable RSSI levels across the three test settings. For instance, at a target RSSI of -60 dBm, the degree of fluctuation follows the trend: Indoor $>$ Corridor $>$ Rooftop. Furthermore, as indicated by the dashed trend lines, open environments tend to have higher and more stable throughput. Throughput on the rooftop remains relatively consistent until the RSSI approaches the receiver sensitivity threshold (–95 dBm for the nRF54L15). In contrast, in complex environments such as the laboratory, a decrease in RSSI results in significantly more rapid degradation in throughput, with a steeper decline compared to the rooftop or corridor scenarios.

Our experimental results demonstrate a strong correlation between RSSI and throughput performance. Generally, the higher the RSSI, the higher the data throughput. However, a given RSSI value alone cannot be used to predict throughput, as different environmental conditions can yield varying results.

Moreover, environmental conditions play a critical role in data throughput. This finding highlights the inherent challenge of maintaining consistent throughput in dynamically changing environments, where signal propagation characteristics and interference levels can fluctuate significantly.

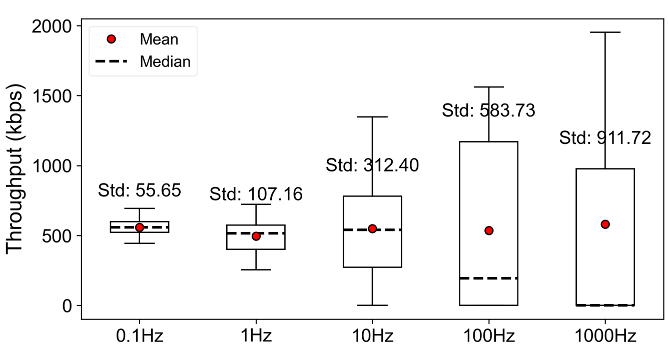

Fig. 3: The mean and standard deviation of throughput under each computation frequency. Higher computation frequencies result in greater fluctuations, while the average values are similar in different cases.

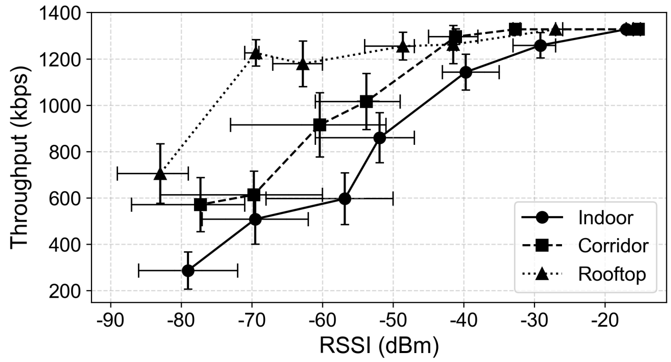

Fig. 4: Comparison of throughput and RSSI in three environments: Indoor, Corridor, and Rooftop. Each point is represented by a box plot of RSSI along the horizontal axis and an error bar indicating throughput along the vertical axis.

B. Power Consumption, Throughput and RSSI with Varying TXP

Figure 5(a) illustrates the power consumption distribution under different TXP settings, using the same communication parameter setup as before. Each black bar presents power measurements at 9 meters indoors to evaluate the impact of TXP on overall power consumption. The corresponding standard deviation is shown by the green error bars. Similarly, in Figure 5(b), the data throughput at each TXP is indicated by the blue bar, and the standard deviation is represented by the red error bars. Figure 5(c) illustrates the impact of adjusting the peripheral TXP on the RSSI measured at the central device.

Figure 5(a) and (b) illustrates an intuitive trend: the higher the TXP, the higher the overall system power consumption, accompanied by increased throughput. However, compared the two parameters, the changes in throughput and power consumption are not perfectly aligned: as the transmit power is increased from –10 dBm to +8 dBm, the power consumption rises from 2.664 mW to 9.18 mW—an almost 3.5 times increase—whereas the throughput only increases from 244.21 kbps to 495.62 kbps, roughly a only twofold increase. This indicates that, while the system's power consumption is positively correlated with throughput, the relationship is not one of direct proportionality.

In previous experiments shown in Figure 4, we observed that throughput varied dramatically with changes in environmental conditions. Generally, to mitigate this issue, TXP should be set at its maximum to maintain a consistent signal strength, as is traditionally done. However, in this experiment, as shown in Figure 5, we found that continuously maintaining a high TXP significantly increased the system's power consumption. At a 9-meter range, the power goes up to 9.18 mW, which is particularly disadvantageous for small, battery-powered devices.

The RSSI in Figure 4 is not directly equivalent to the TXP in Figure 5. Nevertheless, under normal conditions (excluding extreme noise), a higher TXP at the peripheral typically yields a higher RSSI at the central receiver, as indicated in Figure

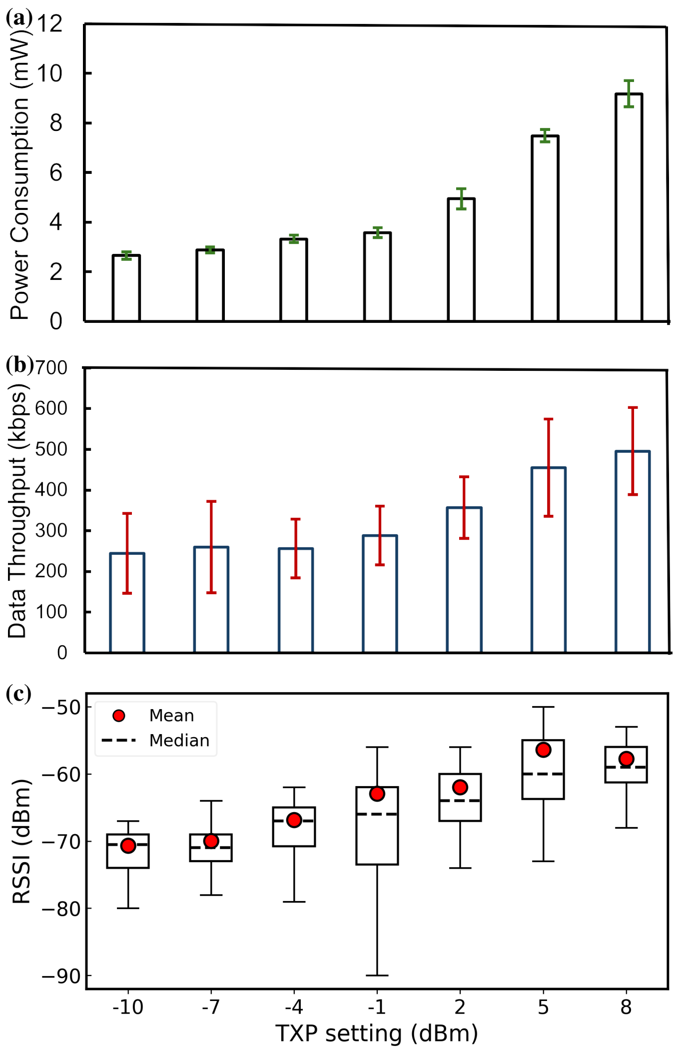

Fig. 5: System power consumption vs. TXP (–10 dBm to 8 dBm) at 9 m indoors (a). Throughput vs. TXP at 9 m indoors (b). Increasing the TXP at the peripheral results in a corresponding increase in RSSI at the central device (c).

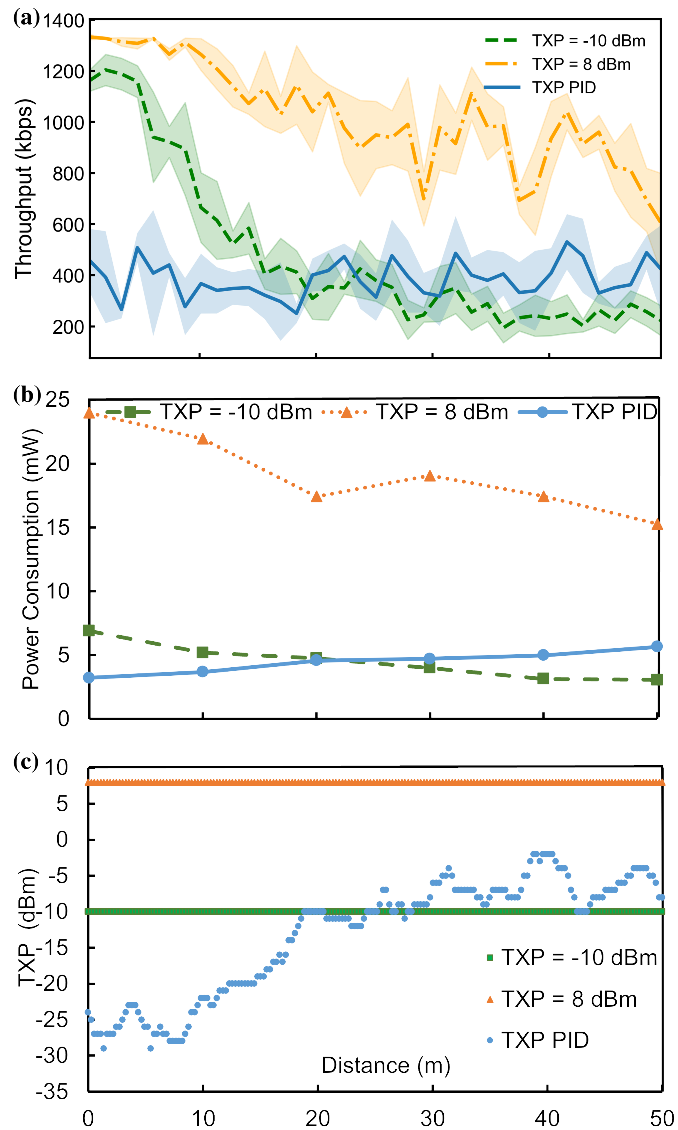

Fig. 6: Variation of throughput (a), power consumption (b), and TXP (c) with increasing distance in a dynamic environment. The PID controller maintains a throughput of around 400 kbps by changing the TXP.

5(c). These experiments suggest that by adjusting the TXP, we can indirectly modify the RSSI and thereby target a throughput to reduce the power issue faced by the traditional method.

Indirectly modulating throughput by adjusting TXP is effective in most cases, particularly in complex environments where RSSI and throughput exhibit an approximately linear relationship. In the indoor laboratory environment shown in Figure 4, the slope between –80 dBm and –20 dBm is about 16 kbps per dBm. Given an adjustable TXP range of 18 dBm, this corresponds to a throughput change of roughly 288 kbps, which closely matches the empirically observed 251.41 kbps reported in Figure 5(b). In this case, users can select a smaller TXP that maintains the target throughput, enabling reduced power consumption.

In contrast, in the low-noise rooftop environment shown in Figure 4, throughput remains consistently above 1,200 kbps across the –70 dBm to –20 dBm range; at this range, TXP adjustments have little impact on throughput. In this scenario, users can select a lower TXP level that still yields an RSSI above –70 dBm at the central device, thus achieving both enough throughput and reduced power consumption. Overall, a TXP control strategy is crucial for balancing throughput requirements with power consumption in various environments.

C. PID Controller Depolyment

Under dynamic conditions, we employed a movable platform at a speed of 0.3 m/s to gradually increase the separation between the central device and peripheral device, simultaneously recording real-time throughput at the central end and real-time power consumption at the peripheral end. The PID and throughput calculations are performed at a rate of 1 Hz.

Figure 6 (a) illustrates the distribution of throughput over distance throughout the entire movement process. The green,

TABLE II: Performance comparison of different TX power control strategies in a dynamic environment (Throughput in kbps, Power in mW)

TX Power Strategy	Average Throughput	STD Throughput	Average Power
-10 dBm fixed	475.94	325.77	4.25
8 dBm fixed	1007.71	224.32	19.08
PID	386.26	132.57	4.34

orange, and blue lines represent TXP fixed at –10 dBm, 8 dBm, and under PID control, respectively. The trend lines include error bands to indicate variability. In both fixed TX power scenarios, throughput exhibits a decreasing trend as the distance increases, primarily due to path loss. In contrast, enabling the PID controller allows the throughput to oscillate around the target of 400 kbps, maintaining performance across varying distances.

In Figure 6(b), we observe the variation in power consumption with increasing distance for three scenarios. Both fixed TXP scenarios (8 and -10 dBm) exhibited a declining throughput trend, primarily due to packet loss. The packet loss introduces idle time between connection events, thereby reducing the system's active communication duty cycle and consequently lowering its average power draw.

In contrast, the PID-controlled scenario adaptively increased power consumption in response to environmental changes as the distance increased. As shown in Figure 6(c), it actively increases its TXP attempting to maintain throughput convergence around the target value of 400 kbps.

The experimental outcomes are summarized in Table II. Results indicate that, with PID control activated, the average throughput converged around 400 kbps, with a minor standard deviation of 132.57 compared to cases with constant TXP of 8 dBm and -10 dBm. Moreover, employing PID control resulted in a reduction in power consumption of approximately 70% compared to continuously maintaining the maximum TXP (8 dBm). In addition, compared with a fixed -10 dBm TXP setting, the PID controller maintained throughput above the application's requirements at the same power consumption level.

This experiment demonstrates the PID controller's capability to regulate throughput by dynamically adjusting the TXP in a changing environment, while dramatically reducing the power consumption.

IV. Conclusion

In this study, we explored the relationship between throughput and RSSI under varying environmental conditions. We observed that environmental variations influence throughput, and we identified a strong correlation between RSSI and throughput, with higher RSSI values associated with increased throughput. Consequently, it is possible to regulate the peripheral device's TXP to achieve a higher RSSI at the central device. However, increasing TXP introduces a trade-off between link quality and energy consumption in different applications, as higher TXP significantly increases power consumption, presenting substantial challenges for low-power applications.

To address this issue, we developed a PID-based control method that computes throughput and applies control at a frequency of 1 Hz. Experimental results demonstrate that this approach effectively maintains the target throughput level with tunable TXP. As a result, it not only meets the application's requirements but also reduces power consumption on the peripheral device side.

This adaptive control mechanism is particularly advantageous in mobile or dynamic BLE environments and power-sensitive applications, such as LE Audio or capsule endoscopy, where maintaining consistent throughput data transmission is crucial without compromising battery life.

V. Acknowledgement

This work was supported by the Nanyang Professorship and the MOE Tier 1 grant RG71/24, as well as the MTC MedTech Programmatic fund M24N9b0125.

References

[1] S. Gautam and S. Kumar, "Low-power ble relay node operation in mesh-like architectures for precision agriculture," *IEEE Sensors Journal*, vol. 24, pp. 33347–33360, 2024.
[2] K. E. Jeon, J. She, P. Soonsawad, and P. Ng, "Ble beacons for internet of things applications: Survey, challenges and opportunities," *IEEE Internet of Things Journal*, vol. PP, pp. 1–1, 04 2018.
[3] G. Koulouras, S. Katsoulis, and F. Zantalis, "Evolution of bluetooth technology: Ble in the iot ecosystem," *Sensors*, vol. 25, no. 4, 2025.
[4] S. A. A. Shah, H. Lee, Y. Jang, and C. Rim, "Iot-integrated ble-based real-time data link and beamforming phased array for healthcare," *IEEE Transactions on Industrial Informatics*, vol. PP, pp. 1–9, 01 2025.
[5] H. Taleb, A. Nasser, A. Guillaume, N. Charara, and E. Cruz, "Wireless technologies, medical applications and future challenges in wban: a survey," *Wireless Networks*, vol. 27, 11 2021.
[6] F. J. Dian, A. Yousefi, and S. Lim, "A practical study on bluetooth low energy (ble) throughput," in *2018 IEEE 9th Annual Information Technology, Electronics and Mobile Communication Conference (IEMCON)*, pp. 768–771, 2018.
[7] W. Wang, H. Sharif, M. Hempel, T. Zhou, and P. Mahasukhon, "Throughput vs. distance tradeoffs and deployment considerations for a multi-hop ieee 802.16e railroad test bed," in *VTC Spring 2008 - IEEE Vehicular Technology Conference*, pp. 2596–2600, 2008.
[8] Bluetooth SIG, Generic Audio Working Group, "Performance Characterization of the Low Complexity Communication Codec." White Paper, June 2023.
[9] J. Tosi, F. Taffoni, M. Santacatterina, R. Sannino, and D. Formica, "Throughput analysis of ble sensor network for motion tracking of human movements," *IEEE Sensors Journal*, vol. 19, no. 1, pp. 370–377, 2019.
[10] E. Park, M.-S. Lee, and S. Bahk, "Adaptable: Data rate and transmission power adaptation for bluetooth low energy," in *2019 IEEE Global Communications Conference (GLOBECOM)*, pp. 1–6, 2019.
[11] E. Salomon and C. A. Boano, "Adaptive transmission power control in ble: Unveiling and overcoming the limits of current solutions," in *2024 20th International Conference on Wireless and Mobile Computing, Networking and Communications (WiMob)*, pp. 455–462, 2024.
[12] D. Halperin, W. Hu, A. Sheth, and D. Wetherall, "Predictable 802.11 packet delivery from wireless channel measurements," *SIGCOMM Comput. Commun. Rev.*, vol. 40, p. 159–170, Aug. 2010.
[13] C.-C. Pu and W. Chung, "Mitigation of multipath fading effects to improve indoor rssi performance," *IEEE Sensors Journal*, vol. 8, pp. 1884–1886, 2008.
[14] Nordic Semiconductor, *nRF54L Series Preliminary Datasheet v0.8*.
[15] Nordic Semiconductor, *nRF52833 Product Specification v1.7*, June 2024.